SLAC-PUB-12122
September, 2006

Tracking code for microwave instability

S. Heifets
Stanford Linear Accelerator Center, Stanford University, Stanford, CA 94309, USA

Abstract

To study microwave instability the tracking code is developed. For bench marking, results are compared with Oide-Yokoya results [1] for broad-band $Q = 1$ impedance. Results hint to two possible mechanisms determining the threshold of instability.

1 Introduction

Longitudinal dynamics of particles in a bunch can be described by the Fokker-Plank equation for the distribution function $\rho(p, x, \tau)$

$$\frac{\partial \rho}{\partial \tau} + \{H(p, x, \tau), \rho\} = \Gamma \frac{\partial}{\partial p}\{\frac{\partial \rho}{\partial p} + p\rho\}, \tag{1}$$

where $x = z/\sigma_0$, $p = -\delta/\delta_0$, and $\tau = \omega_s t$ are dimensionless variables, z is a particle shift in respect to the bunch center, $z > 0$ corresponds to the shift forward, α is the momentum compaction, and $\delta = (E - E_0)/E_0$ is the relative offset in energy. The zero-current rms bunch length σ_0, the rms energy spread δ_0 defined by the synchrotron radiation (SR), and the zero-current synchrotron frequency are related, $\omega_s \sigma_0/c = \alpha\delta_0$. The bunch density $f(x, \tau) = \int dp \rho(p, x, \tau)$ is normalized $\int dx f(x, \tau) = 1$.

In this variables, the right-hand-side of Eq. (1) depends on one parameter $\Gamma = (\omega_s t_d)^{-1}$, where t_d is SR damping time. The Hamiltonian in the Poisson brackets in the left-hand-side (LHS) is

$$H(p, x, \tau) = \frac{p^2}{2} + \frac{x^2}{2} + \lambda \int dx' f(x', \tau) S[\sigma_0(x' - x)], \tag{2}$$

Presented at ILC DR Workshop, Cornell , 26-28 September 2006, Ithaka, NY, USA

Work supported by Department of Energy contract DE-AC02-76SF00515

where $S(z)$ is given by the longitudinal wake per turn $S(z) = \int_0^z dz' W(z')$, and

$$\lambda = \frac{N_b r_e}{\gamma \alpha \delta_0^2 C}. \tag{3}$$

Here N_b is bunch population,γ is the relativistic factor, r_e is the classical electron radius, and C is the ring circumference. The positive wake means energy loss. In the ultra-relativistic case, $W(z) = 0$ for $z < 0$.

Eq. (1) has the steady-state (Haissinski) solution $\rho \propto e^{-H}$. In the variables x, p the rms $\langle x^2 \rangle = \langle p^2 \rangle = 1$.

The LHS of Eq. (1) corresponds to the the system of equations of particles motion

$$\begin{aligned} \frac{dx_i}{d\tau} &= p, \\ \frac{dp_i}{d\tau} &= -x_i + \lambda \sigma_0 \sum_j W[\sigma_0(x_j(\tau) - x_i(\tau))], \end{aligned} \tag{4}$$

while the RHS describes diffusion and SR damping.

Actually, the LHS of the Fokker-Plank equation is only an approximation to Eqs. (4) which,generally speaking, contain higher-order particle correlations neglected in Eq. (1).

Usually, the threshold of instability can be defined neglecting the RHS of the Fokker-Plank equation and linearizing the LHS around the steady-state solution.

Alternative approach is tracking, i.e. solution of Eq. (4) for a number of macro particles $i = 1, 2, .., M$, where M has to be sufficiently large but still $M << N_b$. Tracking is a standard method to study beam dynamics. It was used before to study microwave instability by K. Bane and K. Oide [2] and by K. Oide and K. Yokoya [1].

In simulations, equations of motion for macro-particles are solved with a time step $\delta\tau$. At each time step, equations are replaced by the transform $(p, x) -> (\bar{p}, \bar{x})$

$$\begin{aligned} \bar{p}_i &= p_i + \delta\tau(-x_i + \lambda\sigma_0 \sum_j W[\sigma_0(x_j(\tau) - x_i(\tau))] - \delta\tau\, \Gamma\, p_i + a \sum_{k=1}^{n_k} \xi_k, \\ \bar{x}_i &= x_i + \delta\tau\, \bar{p}. \end{aligned} \tag{5}$$

Here ξ_k is a random variable uniformly distributed in the interval $-1 < \xi < 1$. The term proportional to ξ_k is introduced to describe diffusion of the RHS of Eq. (1) with the rate $d < p^2 > /d\tau = 2\Gamma$. That defines the coefficient $a = \sqrt{6\Gamma/\dot{n}_k}$ where the rate $\dot{n}_k = n_k/\delta\tau$ depends on the number of random kicks n_k applied at each time step. For a single kick, $n_k = 1$, and $a = \sqrt{6\Gamma\delta\tau}$.

Parameter Γ defines both damping and diffusion rates. The map Eq. (5) is simplectic if $\Gamma = 0$.

Simulations are faster if the sum over macro-particles $W[\sigma_0(x_j(\tau) - x_i(\tau))]$ in Eq. (5) is replaced by the integral

$$\int dx' f(x',\tau) W[\sigma_0(x' - x_i(\tau))], \tag{6}$$

where $f(x,\tau)$ is defined on each time step by interpolating the actual distribution of macro-particles on a mesh centered at the bunch centroid.

The FORTRAN code was generated utilizing Eqs.(5),(6). The code starts with calculations of the steady-state Haissinki distribution $\rho(x,p)$ using Newton's iteration method suggested by R. Warnock. The loop over the bunch current starts from a low current and use obtained Haissinski distribution as starting function for the next higher value of the current. Then, coordinates $\{x_i, p_i\}$ of M macro-particles are generated with the probability given by $\rho(x_i, p_i)$. After that, the tracking starts for specified number of time steps n_m. The code stops when the calculated rms energy spread exceeds some specified value δ_{max} or number of steps exceeds n_m. In the first case, the current is taken as the threshold of instability. In the later case, the process is repeated with the higher value of current.

2 Results

Simulations were carried out, for bench mark purpose, with the broad-band $Q = 1$ resonator wake. In this case, there are only two independent parameters given by the resonance frequency ω_r and the shunt impedance R_s,

$$x_r = \frac{\omega_r \sigma_0}{c}, \quad S_r = \frac{I_{bunch} r_e}{ec} \frac{4\pi\omega_r}{\gamma\omega_s\delta_0} \frac{R_s}{Z_0}, \tag{7}$$

where $Z_0 = 120\pi$ Ohm.

The results were checked with different time steps. For the time step less that $\delta\tau < 0.5$ calculations are stable. For example, the threshold $S_r = \{9.22, 9.32, 9.22\}$ for $\delta\tau = \{0.25, 0.125, 0.0625\}$, respectively. Calculations give results independent on the number of random kicks per time step.

Normally, we use the time step $\delta\tau = 0.125$ (50 steps per synchrotron period), one random kick per time step, the damping time $\Gamma = 1.\,10^{-2}$, and the number of time steps 8000 corresponding to 10 damping times. Interpolation of macro-particle distribution over x is carried out on the 101 bins mesh with the mesh size $-10 < x < 10$. At large bunch currents, the bunch distribution usually is tilted forward. Respectively, the mesh is redefined to keep the maximum of the distribution at the mesh center. The average CPU time is $1.1\,\mu s$ on 2.4 GHz PC. For each x_r, the threshold S_r was found increasing S_r by steps, usually, $\delta S_r = 0.5$.

The results of simulations are shown in Fig. (1)-(3). In Fig. (1) we compare Oide-Yokoya and our results for $1.\,10^4$ and $5.\,10^4$ macro-particles. Fig. (2) results are compared for two damping times: $\Gamma = 10^{-2}$ (red), and Γ reduced by the factor (1/3) (blue).

Fig. (1) shows that the tracking results deviate from the curve predicted by Oide-Yokoya at large $x_r > 0.5$ in agreement with their own tracking results. It was suggested before (P. Wilson, private communication) that the threshold of the microwave instability is related to appearance of a new minimum of the Haissinski steady-state potential. In Fig. (3) we plot Oide-Yokoya result (blue line) and the threshold S_r at which the Haissinski potential $U_H(x)$ has two minima. The threshold for the second minimum is defined searching equation $dU_H/dx = 0$ for an additional root. The length of the bars in Fig. (3) gives the distance of the new minimum from the bunch center. The additional minimum (double horn Haissinski distribution) at small x_r appears in the tail of the distribution. However, for larger x_r the minimum shifts toward the bunch center and, at large $x_r > 0.5$, the conjecture seems to be valid: the threshold of instability found by tracking deviates from the Oide-Yokoya theory following the curve of the new minimum. The crossings takes place around $x_r = 0.5$.

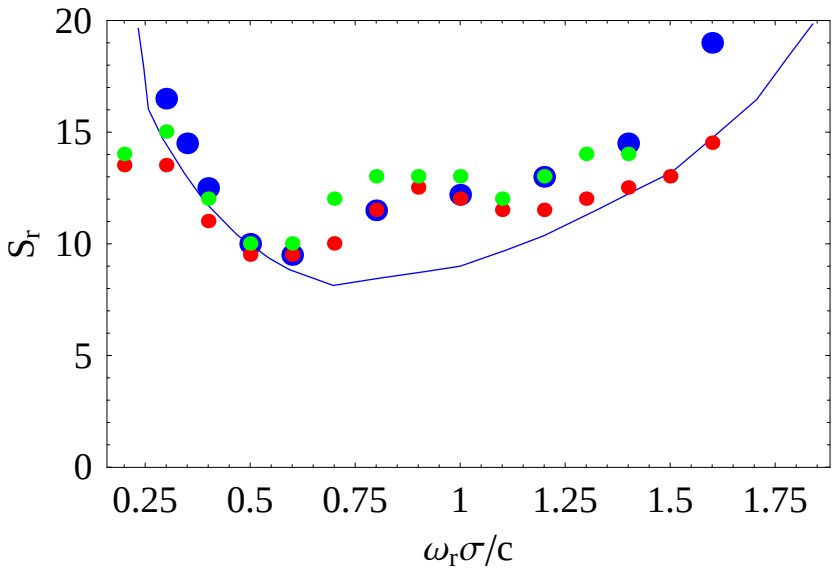

Figure 1: The threshold of the microwave instability for $Q = 1$ impedance. The result of Oide-Yokoya theory is shown by blue line and their own tracking results by large blue dots. Our calculations are shown by small dots: for 10^4 macro-particles in green, and for $5.\,10^4$ macro-particles in red. A single point means that two points are overlap.

The main uncertainty in defining the threshold of instability δ_{th} comes from the uncertainty of the criterion $\delta_{th} > \delta_{max}$. The microwave instability does not lead to exponential growth but to increasing energy spread and, sometimes, to saw-tooth modulation of the rms bunch length. Because the energy spread close to the threshold grows slowly and δ in tracking fluctuates, the threshold is smeared. This problem can be elevated using large number of macro-particles what requires larger CPU time. In simulations we use

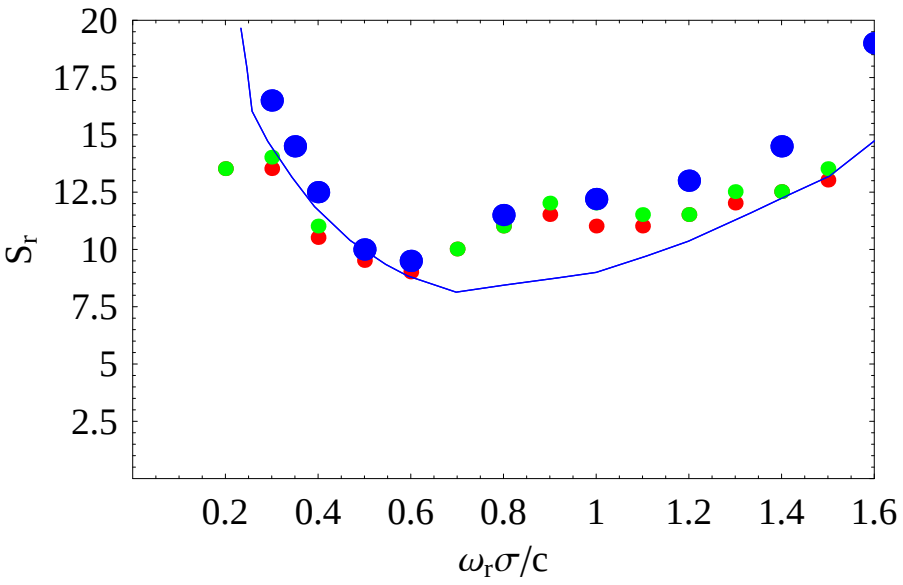

Figure 2: Dependence of the threshold on the damping time. Results of Oide-Yokoya are shown in blue. Our calculations are shown by small dots for two damping times: $\Gamma = 10^{-2}$ (red), and $\Gamma = (1/3)\,10^{-2}$ (green).

$\delta_{max} = 1.1$ (Oide and Yokoya used $\delta_{max} = 1.05$).

In Figs. (4)-(8) we study the dynamics of instability in more details. Fig. (4) is an example of the dynamics at small $x_r = 0.3$ above the threshold of instability. Calculated are the average over macroparticle distribution $< x >$, $< p >$, rms energy spread δ, and the spectrum of $\delta(\omega)$. The spectrum is shown as function of the number i related to the frequency $\omega_i = 2\pi(i-1)/(n_s\delta\tau)$, where $n_s = 16000$ is the number of records and $\delta\tau = 0.125$ is the time step (each 5-th step is recorded). Note, that $< x >$, $< p >$, and δ all show the saw-tooth behavior. Fig. (5) shows that such behavior at small x_r appears only above the threshold of the instability. Comparing behavior for $x_r = 0.3$ and $x_r = 0.4$ in Fig. (6) we see that the period and amplitude of saw-tooth kinks decreases for x_r approaching the crossing point $x_r = 0.5$. Parameters S_r in both cases were chosen to be approximately above the threshold of instability on the same amount. Fig. (7) shows that the amplitude and repetition rate of the saw-tooth kinks depend on the damping time. All that is consistent with the Baartman-Dyachkov [3] mechanism of instability. In terms of the mode analysis, similar behavior can be obtained close to the threshold as result of the nonlinear interaction of few unstable mode [4].

For large x_r above the crossing the dynamics is quite different. Fig. (8) show the time variation of the rms energy spread at $x_r = 0.8$ for two currents above the threshold of instability. The bunch temperature increases, $\delta > 1$ with S_r above the threshold, but there is no evidence of the saw-tooth instability. That is consistent with the smaller

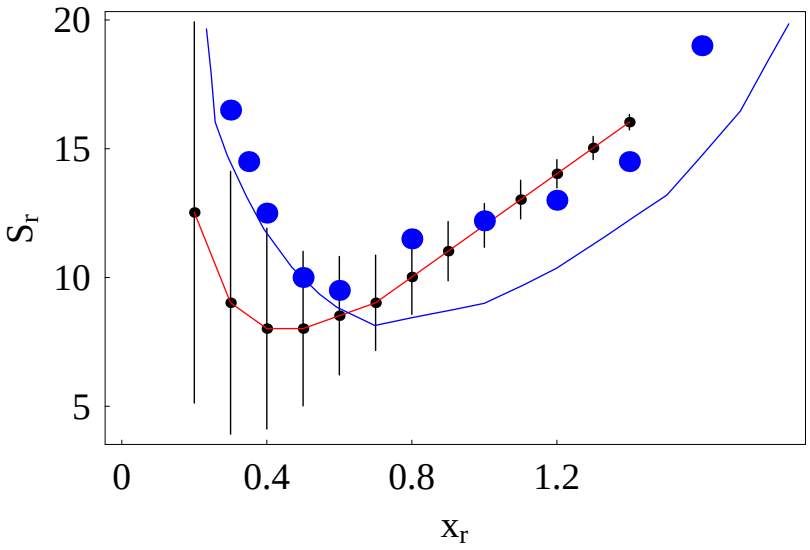

Figure 3: Comparison of the threshold of the microwave instability (blue line) with the threshold of two-minima Haissinski potential well. The total length of the bar is the distance Δx to the additional minimum. Both curves tend to coincide at $x_r > 0.5$ while for smaller x_r the second minimum is on the far tail of the distribution and does not cause the instability.

separation of the two minima of the Haissinski potential for large x_r.

References

[1] K. Oide and K. Yokoya, Longitudinal Single-Bunch Instability in Electron Storage Rings, KEK Preprint 90-10, April 1990, A

[2] K. Bane and K. Oide, Proc. of the 1993 IEEE Particle Acc. Conf., Washington D.C., 1993, p. 3339

[3] R. Baartman. and M. Dyachkov, M. Proc. IEEE Part. Accel. Conf., Dallas, 1995.

[4] S. Heifets, Nonlinear mode coupling and saw-tooth instability, SLAC-PUB-8242, Spetember 1999

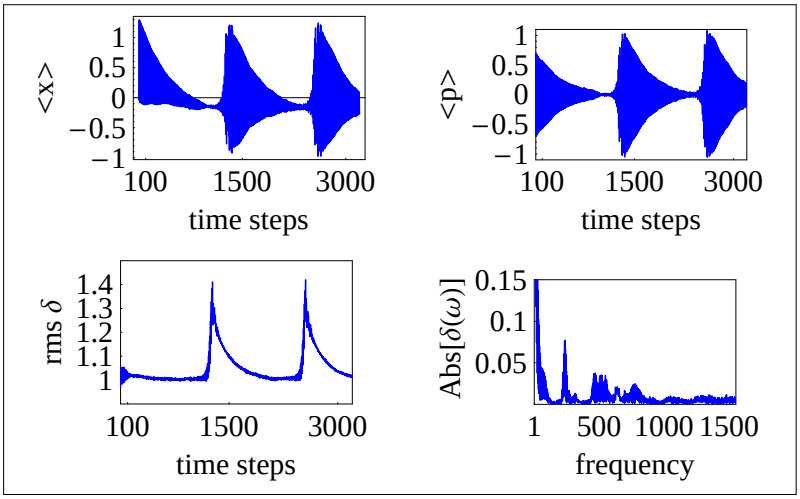

Figure 4: Dynamics of the microwave instability above threshold, $x_r = 0.3$, $S_r = 13.84$, $\Gamma = 1.0\,10^{-2}$. Total number of time steps 16000 with $\delta\tau = 0.125$ (each 5-th step is recorded). The total time of tracking $t/t_d = 10$.

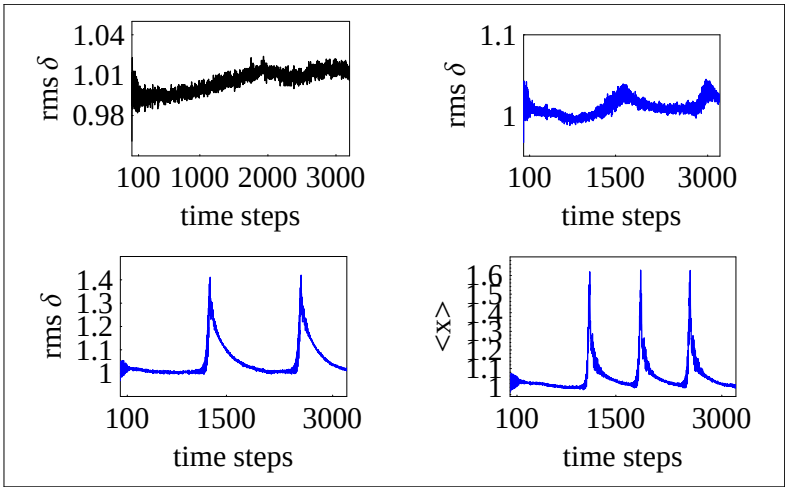

Figure 5: Dependence of the saw-tooth behavior on current. $x_r = 0.3$, Top row: $S_r = 11.74$ (left), 12.84 (right), bottom row: 13.84 (left), and 14.84 (right). Other parameters are the same as in Fig. (4).

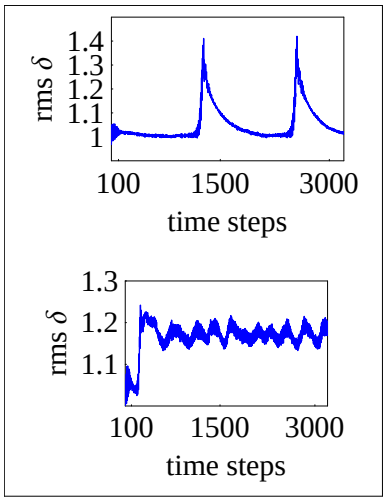

Figure 6: Time dependence of the rms energy spread above the threshold of microwave instability for $x_r = 0.3$, $S_r = 13.84$ (top) and $x_r = 0.4$, $S_r = 12.02$ (bottom). Other parameters are the same as in Fig. (4).

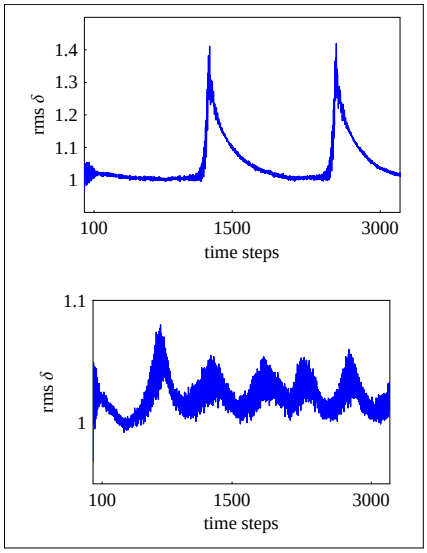

Figure 7: Effect of the damping time on the time variation of the rms energy spread above the threshold of microwave instability. $\Gamma = 1.0\,10^{-2}$ (top) and $\Gamma = 3.0\,10^{-2}$ (bottom). Other parameters the same as in Fig. (4).

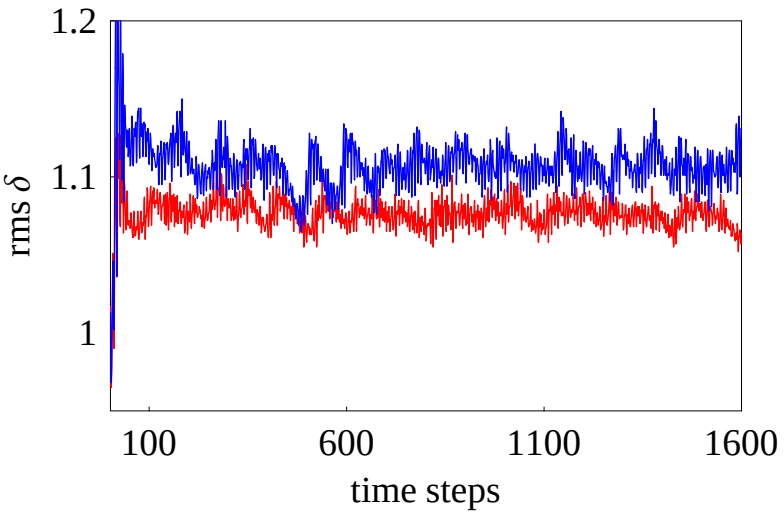

Figure 8: Time dependence of the rms energy spread above the threshold of microwave instability for large x_r. $S_r = 11.8$ (red), $S_r = 13.02$ (blue), in both cases $x_r = 0.8$. (4).